Effectiveness of fluorine termination at nitrogen vacancies inside gallium nitride crystals based on first-principles calculations

Yuki Fujishiro[1*], Tomoe Yayama[2*], Takahiro Nagata[3], Toyohiro Chikyow[4], Fumiko Akagi[1, 2]

[1] Electrical Engineering and Electronics Program, Graduate School of Engineering, Kogakuin University, Shinjuku-ku, Tokyo 163-8677, Japan

[2] Department of Applied Physics, School of Advanced Engineering, University of Kogakuin, 1-24-2, Nishi-shinjuku, Shinjuku-ku, Tokyo, Japan

[3] Research Center for Electronic and Optical Materials, NIMS, 1-1 Namiki, Tsukuba, Ibaraki 305-0044, Japan

[4] Research Center for Materials Nanoarchitectonics (MANA) Center for Basic Research on Materials, NIMS, Tsukuba, Japan

* Authors to whom correspondence should be addressed: cm24041@ns.kogakuin.ac.jp; yayama.tomoe@cc.kogakuin.ac.jp

ABSTRACT

Nitrogen (N) vacancies inside gallium nitride (GaN) crystals can scatter carriers and degrade the performance of GaN-based devices. Hydrogen (H) termination is an effective approach for eliminating defect levels in Si crystals but is less effective for GaN because the latter requires higher processing temperatures, which causes H to desorb more easily. Fluorine (F) is a potential alternative to H owing to its high chemical reactivity and small atomic radius. In this study, first-principles calculations were used to investigate the effectiveness of F termination at N vacancies in GaN crystals. The calculated density of states and band dispersion diagram indicated that F termination eliminated defect states near the conduction band edge and made the electronic states near the band edges resemble those of intrinsic GaN. These effects were attributed to the bonding of F atoms with Ga dangling bonds. Although H termination also resulted in the bonding of H atoms with Ga dangling bonds, the bonding states remained within the bandgap near the band edges; therefore, defect levels were not eliminated as effectively as with F termination. This behavior was attributed to the larger energy difference between the bonding and antibonding states of Ga–F bonds compared with Ga–H bonds. These results suggest that F termination can eliminate defect levels caused by N vacancies inside GaN crystals and improve the performance of GaN-based devices.

I. INTRODUCTION

Gallium nitride (GaN) is a semiconductor with excellent carrier mobility and dielectric breakdown strength.[1,2] However, defects that form during the fabrication of a GaN-based device can result in defect levels in the bandgap and near the band edges, which can cause problems such as current collapse.[3,4] Eliminating these defect levels can improve the reliability of GaN-based devices. Defect levels in Si crystals[5] and Si–SiO_2 interfaces[6] are typically eliminated by hydrogen (H) termination. The effectiveness of annealing is determined by the annealing temperature, but annealing GaN typically requires higher temperatures because of its higher melting point compared with Si. For example, Si requires an annealing temperature of 800°C–1000°C to restore crystallinity after ion implantation[7,8] while GaN requires an annealing temperature of about 1100°C–1400°C.[9,10] In addition, a temperature that is approximately two-thirds the melting point (in Kelvin) is generally required for recrystallization during annealing.[11,12] At higher temperatures, adsorbed H desorbs more easily[13,14] and can passivate acceptors by forming complexes in Mg-doped p-type GaN.[15-17] Therefore, a termination element other than hydrogen, one that remains adsorbed even under high-temperature annealing, is needed to eliminate defect levels in GaN crystals.

One potential alternative is fluorine (F). Jung et al.[18] investigated the effectiveness of F termination for Germanium (Ge) and confirmed a decrease in vacancy concentrations. F has the highest electronegativity among all elements and thus has high chemical reactivity, which would help keep F atoms bonded on Ga atoms. Furthermore, F atoms have a small atomic radius, which should allow them to diffuse easily inside GaN crystals. To date, the incorporation of F into GaN crystals has been achieved via ion implantation, and the stability of F atoms in GaN crystals and at AlGaN–GaN interfaces has been investigated.[19,20] Based on hard X-ray photoelectron spectroscopy measurements at SPring-8, Nagata et al. reported that the Fermi level of GaN thin films annealed under various fluoride atmospheres shifted to the valence band after fluorination unlike untreated samples. This shift suggests that the incorporated fluorine compensates for the residual charges in GaN by reducing the density of defects responsible for Fermi-level pinning.[21,22] Gao et al. reported that F plasma treatment of AlGaN/GaN high-electron-mobility transistors reduced the leakage current, which may be attributed to a decrease in interface traps.[23] Using first-principles calculations to determine the electronic state of the GaN surface during the adsorption of several F atoms, we previously found that F atoms effectively terminated the GaN (0001) surface.[24] Thus, F termination was confirmed to eliminate surface levels from the bandgap at the GaN surface. However, defects that are critical to GaN-based device performance are not necessarily located at the surface but at the interfaces of nitride heterojunctions or inside GaN crystals, where there is marginal space for adsorbed atoms. Therefore, it is necessary to clarify the effects of F termination on defects inside GaN crystals.

In this study, we focused on N vacancies inside GaN crystals and used first-principles calculations to investigate how F atoms are adsorbed onto Ga dangling bonds caused by N vacancies inside a GaN

crystal and to determine their stable atomic configurations. We then analyzed the electronic states of the obtained adsorption structures to clarify whether and how defect levels were eliminated. We also examined the differences between F and H terminations.

II. METHODS

The electronic states were obtained via first-principles calculations based on density functional theory using the Vienna Ab initio Simulation Package.[25-28] The generalized gradient approximation of Perdew–Burke–Ernzerhof (GGA-PBE) was used as the exchange-correlation functional.[29-31] For structural optimization, the convergence criterion was set to 0.005 eV/Å. For the calculations, a cutoff energy of 800 eV and 4 × 4 × 4 k-points mesh were applied. The lattice constants, c/a ratio, and atomic positions were optimized for a GaN unit cell containing two N atoms and two Ga atoms. The optimized lattice constants were a = b = 3.22 Å and c = 5.25 Å. Several types of 3 × 3 × 3 GaN supercell models were created with this unit cell: a pristine model without any defects (i.e., defect-free model), a model incorporating a single N vacancy (V_N i.e., defect model), and defect-containing models in which the vacancy was terminated by F or H atoms in various configurations. In this study, we focused on models in which three F atoms were adsorbed (i.e., F-terminated). We also considered models in which three H atoms were adsorbed for comparison (i.e., H-terminated). The metastable structures and electronic states were then determined for each model. We validated the cell size dependency by visualizing the charge density distribution for different supercell dimensions. The results confirmed that localized bonding states in F-terminated model were effectively contained within both the 3 × 3 × 3 model and larger models and that these models reproduced equivalent bonding states.

As a preliminary calculation, formation energies were calculated for models in which one to four F atoms were placed around a N vacancy. The metastable structure with three F atoms placed around the N vacancy had the lowest formation energy over a wide range of both the chemical potential parameters of F and the Fermi level shift (Supplementary Materials). Furthermore, we confirmed that the thermodynamic stability of the charged states of V_N was consistent with the work reported the formation energy of GaN with the various types of defect by Lyons and van de Walle.[32] According to the electron counting model,[33] the stability of these F terminated models is because the number of electron pairs derived from the bonding between the Ga dangling bonds and F atoms is an integer.

III. RESULTS AND DISCUSSION

A. Identification of metastable structures

The optimal structures of the defect-free, defect, F-terminated, and H-terminated models were identified, and the stable positions of F and H atoms near the N vacancy were determined.

1. Defect-free and N-vacancy models

Figure 1(a) shows an overall view of the defect-free model, which is a GaN 3 × 3 × 3 supercell containing 54 Ga atoms and 54 N atoms. Fig. 1(b) and (c) show enlarged views of a part of the defect-free model and the defect model in the area near a N vacancy. Both models were structurally optimized. In the defect-free model, the bond lengths along the a–b plane and c-axis are 1.97 and 1.98 Å, respectively. In the defect model, these bond lengths are 1.93 and 1.96 Å, respectively. Therefore, the Ga atoms adjacent to the defect move toward the N vacancy. The defect model has dangling bonds on the four Ga atoms adjacent to the N vacancy due to four broken Ga–N bonds that can interact with exogenous species.

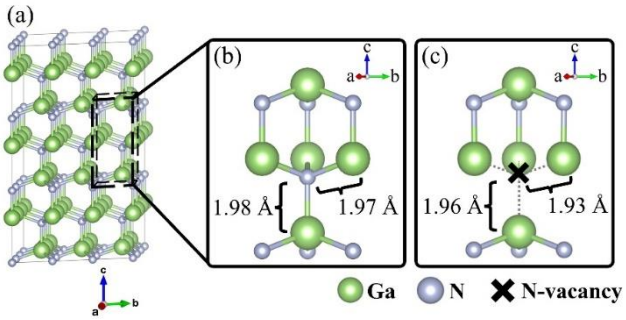

Fig. 1. Defect-free and defect models: (a) overall view of the defect-free model, (b) enlarged view of the defect-free model, and (c) enlarged view of the N vacancy in the defect model.

2. Fluorine-terminated models

To determine the energetically stable positions for adsorption of F atoms onto Ga dangling bonds, our approach involved a two-step geometry analysis. First, we detected the potential energy surface (PES) via atomic probing with F and H atoms. Second, we optimized the geometry using the conjugate gradient (CG) method. We employed this two-step analysis because simple geometry optimization only yields results that converge to the local minimum nearest the initial atomic configuration. Exploration of the PES is effective for determining the number and stability of various metastable structures that may exist in the vicinity of the defect. To restrict the degrees of freedom in the exploration, the atomic configuration was fixed during this procedure and the position of the probe atom was varied one-dimensionally. As a first step, total energies were evaluated for F-terminated models with three F atoms placed at various points near the N vacancy. As shown in Fig. 2(a), the line connecting a Ga atom and the N vacancy can be defined as an r-axis, where the N vacancy is positioned at $r = 0$. Because four Ga atoms neighbor the N vacancy, four corresponding r-axes can

be defined. As shown in Fig. 2(b), an axis connecting the N vacancy and atomic position A can be defined as r_A, and the other axes connecting the N vacancy to atomic positions B, C, and D can be defined as r_B, r_C, and r_D, respectively. The F atoms can then be placed along these axes. For simplicity, the values of r_i (i = A to D) are set the same for all axes rather than setting each independently. Accordingly, r_i is denoted simply as r hereafter. Positions with $r < 0$ are closer to the Ga atom, whereas those with $r > 0$ lie in the direction opposite the Ga atom. The F-terminated model with F atoms placed at three of these four positions is designated as the F3 model. In terms of symmetry, two distinct patterns can be defined depending on which three of the four axes the F atoms are placed along. For pattern 1 (p1), F atoms are placed along r_B, r_C, and r_D. For pattern 2 (p2), F atoms are placed along the axes r_A, r_C, and r_D. Two additional configurations equivalent to p2 are also possible, with F atoms located at A, B, and C or at A, B, and D.

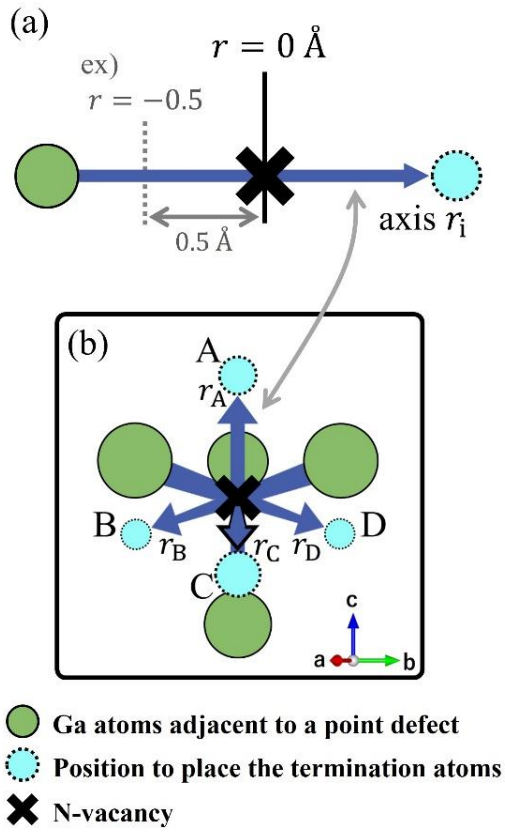

Fig. 2. Definition of the axis r: (a) position of a F atom on axis r_i (i = A–D), and (b) axis r_i in real space.

Fig. 3 shows the relationship between the total energy and F atom position r for the F3p1 and F3p2 models, where the F atoms are placed at 0.1-Å intervals in the ranges $-1.5 \leq r \leq -0.5$ and $0.5 \leq r \leq 2.5$. Both the F3p1 and F3p2 models have two local minima in the negative and positive r

regions. The local minimum in the positive region ($r = 1.3$ Å) has a lower energy than the local minimum in the negative region. In other words, a structure in which the F atoms are located away from the Ga atoms rather than close to them is more stable.

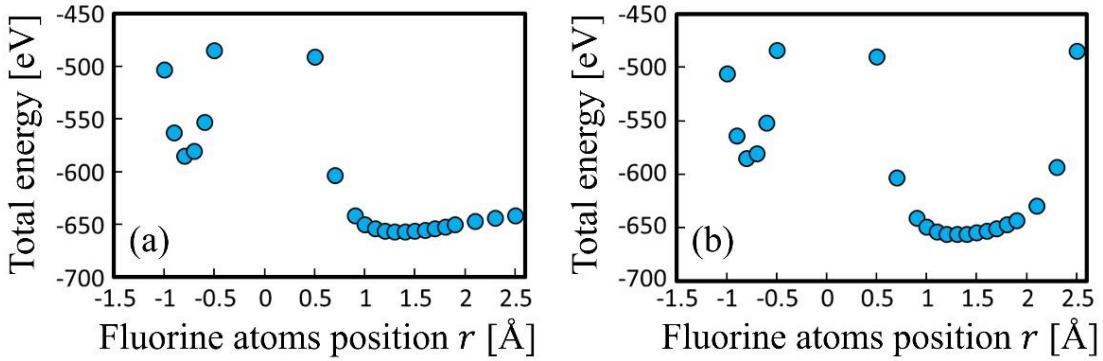

Fig. 3. Relationship between the F atom position r and total energy of F3 models: (a) F3p1 and (b) F3p2.

As a second step of geometry analysis, we performed structural optimization using CG method for F3p1 and F3p2 using the three lowest-energy structures in the positive r region as initial configurations. The three initial structures of F3p1 relaxed to the same metastable configuration, referred to as F3p1_opt. Similarly, the three initial structures of F3p2 relaxed to the same metastable configuration, referred to as F3p2_opt. F3p2_opt had a lower total energy (−659.315 eV) than F3p1_opt (−658.722 eV), indicating that F3p2_opt represents the most stable adsorption structure. Fig. 4 shows the initial and optimized structures of F3p2_opt around the N vacancy. The F atom originally at point A (Fig. 4(a) and 4(b)) moves away from the other F atoms (red arrow) to a position between the Ga atoms in the optimized structure (Fig. 4(c) and 4(d)). These results indicate that the F atoms adsorb on the Ga dangling bonds while maintaining distance from each other. F3p2_opt appears to represent a stable configuration for terminating Ga dangling bonds with three F atoms.

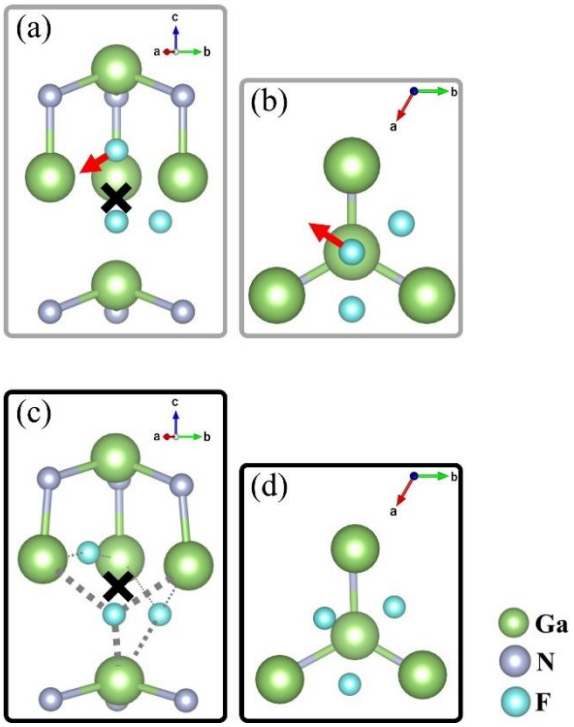

Fig. 4. F3p2_opt model: (a) enlarged view (b) and parallel view along the *c*-axis of the initial structure; (c) enlarged view and (d) parallel view along the *c*-axis of the optimized structure.

3. Hydrogen-terminated models

A stable structure was determined for H-terminated models in the same manner as for the F-terminated models discussed in the previous section. Because H is a monovalent element similar to F, termination by three H atoms (i.e., H3 model) also satisfies the electron counting model. As with the F3 model, the H3 model also had two distinct patterns: H atoms placed along r_{B}, r_C, and r_{D} (p1) and H atoms placed along r_{A}, r_C, and r_{D} (p2). For both patterns, H atoms were placed at 0.1-Å intervals in the ranges of $-1.5 \leq r \leq -0.3$ and $0.5 \leq r \leq 2.5$. Fig. 5 shows the relationship between the energy and H atom position r. Both the H3p1 and H3p2 models exhibited local minima in the negative and positive r regions. However, the energy difference between the local minima in the negative and positive regions was smaller for H than for F.

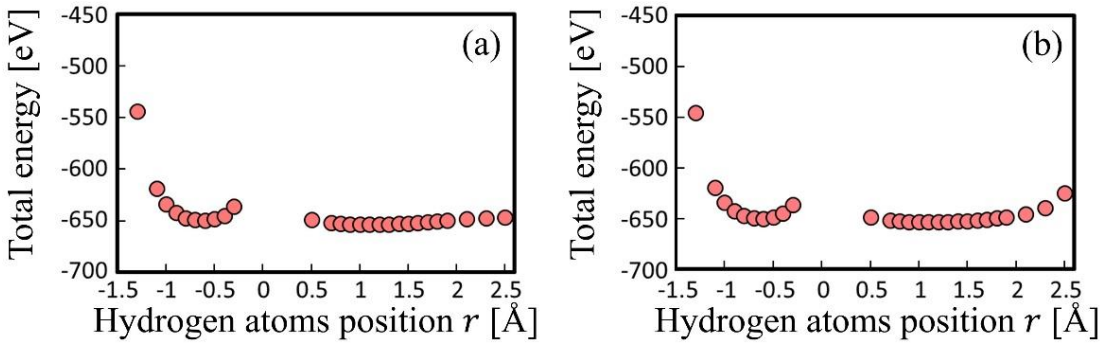

Fig. 5. Relationship between the H atom position r and total energy of H3 models: (a) H3p1 and (b) H3p2.

For both the H3p1 and H3p2 models, as a second step of geometry analysis, CG geometry optimization was performed using the three different structures near the minimum energy as initial configurations. We confirmed that the same metastable structure was obtained at each energy minimum. Table I lists the energies of the metastable structures. The most stable structure was generated when the H3p2 model with H atoms placed in the negative r region was used as the initial configuration (H3p2_opt).

Table I. Total energies of metastable structures for the H3p1 and H3p2 models.

	Negative r	Positive r
H3p1	−653.422 eV	−654.146 eV
H3p2	**−654.667 eV**	−654.347 eV

Fig. 6 shows an enlarged view around the N vacancy for the H3p2_opt model. Two H atoms are located on the upper side where the Ga atom density is higher, and one H atom is positioned on the lower side. Throughout the two-step geometry analysis, we found that the PES exhibits one local minimum on each side of the defect for F and H probe atoms. This finding was further confirmed via CG geometry optimization starting from multiple initial configurations near these local minima, which consistently converged to the same final structures. Furthermore, the stable configuration exhibited a clear elemental dependence: the local minimum further away from the Ga atom is more stable for F whereas the local minimum closer to the Ga atom is more stable for H. Although F and H are monovalent elements, we found that their stable structures are different, which may due to their ionic radii difference.

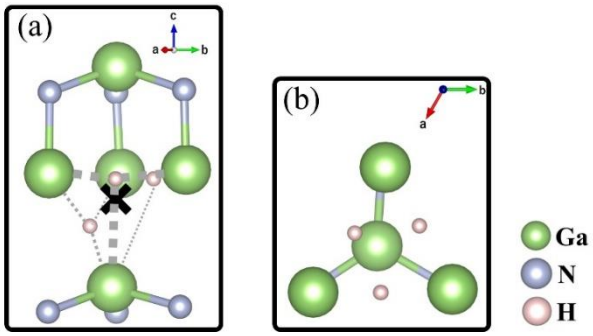

Fig. 6. H3p2_opt model: (a) enlarged view and (b) parallel view along the c-axis.

B. Electronic states

The electronic states for F3p2_opt and H3p2_opt were determined. Fig. 7 shows the band dispersion diagrams and density of state (DOS) distributions for the (a) defect-free, (b) defect, (c) F3p2_opt, and (d) H3p2_opt models. The highest occupied state was set to 0 eV. Both the total DOS and projected DOS (PDOS) were determined for each model. The PDOS includes the outermost orbitals, which include the 4p orbitals of the four Ga atoms adjacent to the N vacancy, the 2p orbitals of the F atoms, and the 1s orbitals of the H atoms. The band dispersion diagrams of the defect-free and defect models show that the latter has a band near the conduction band minimum (CBM) at approximately 0.5 eV that does not appear in the former. This band has marginal energy dispersion, which indicates that it is a localized state. Although the nearly flat defect-induced band exists within the conduction band, the location is considerably shallow and likely serves as a trap level, such as for optical devices under finite temperature and especially highly band-filling conditions. [34] The presence of defect-induced level near the CBM is consistent with the results reported by Lewis et al., who analyzed the electronic states using HSE06 and found defect levels located at CBM +0.2 eV to CBM +0.42 eV.[35]The PDOS of the defect model also has a peak for Ga_4p near the CBM, which indicates that the previous localized state derives from the Ga dangling bonds. The band dispersion diagram of the F3p2_opt model has clear band edges and no defect levels near the valence band maximum (VBM) and CBM, and it is more similar to the defect-free model than the defect model. In the PDOS of the F3p2_opt model, the peak for Ga_4p no longer exists near the band edges. The lower panel of Fig. 7(c) shows states consisting of Ga_4p and F_2p at approximately −7.5 eV below the VBM. This suggests that three F atoms passivate the Ga dangling bonds and form bonding states, which consequently pushes the corresponding defect levels far from the band edges. The bonding state at Γ point is further discussed in the following section based on the charge density distribution.

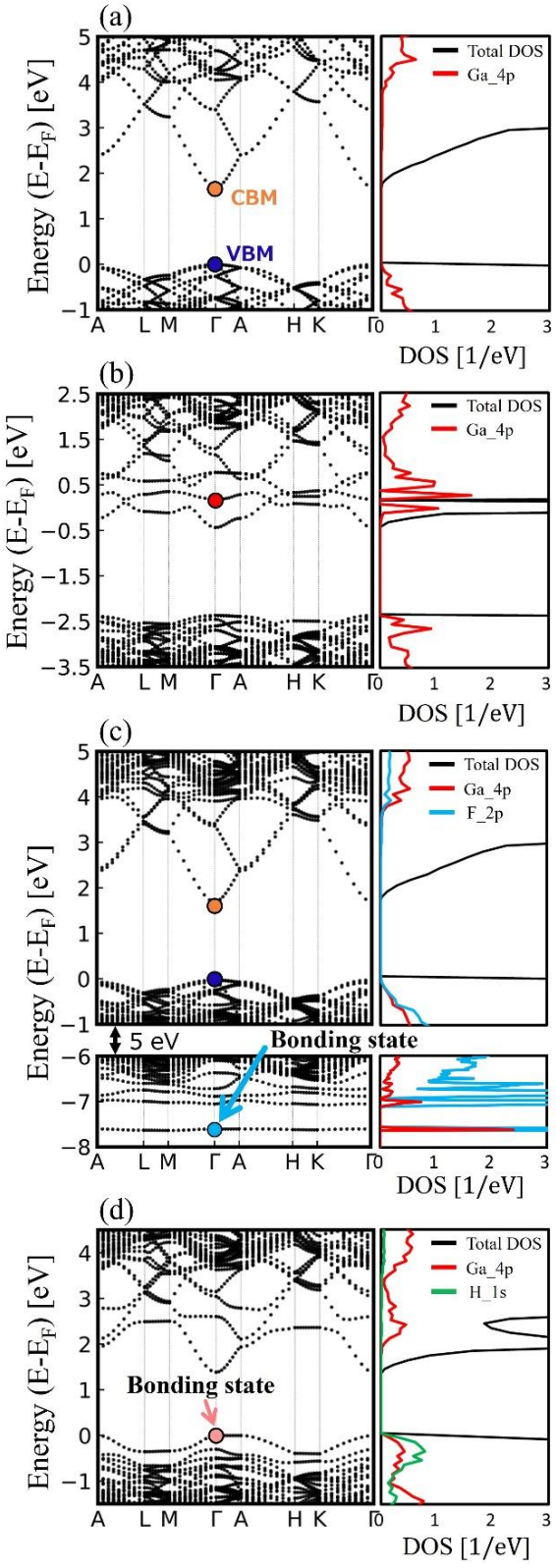

Fig. 7. Band dispersion diagrams and density of state (DOS) distributions: (a) defect-free model, (b) defect model, (c) F3p2_opt model, and (d) H3p2_opt model.

Figs. 8–11 show the charge density distributions for the defect-free, defect, F3p2_opt, and H3p2_opt models, respectively. Fig. 8(a) shows that the charge density of the CBM in the defect-free model forms an s-orbital-like isosurface enclosing the N atoms. Fig. 8(b) shows that the charge density of the VBM in the defect-free model forms a p-orbital-like isosurface enclosing the N atoms. Fig. 9 shows the charge density distribution of the defect model at the Γ point (red point in Fig. 7(b)), which is considered to be a defect level. The charge density is localized around the Ga atoms adjacent to the N vacancy, which confirms that the states observed near the CBM are due to Ga dangling bonds.

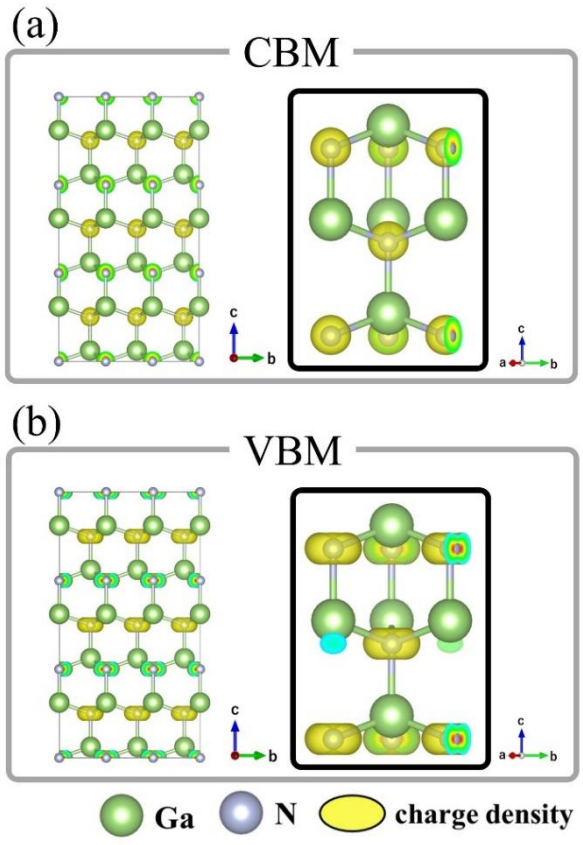

Fig. 8. Charge density distributions of the defect-free model: (a) CBM and (b) VBM. The isosurface values were taken to be 0.001/bohr^3.

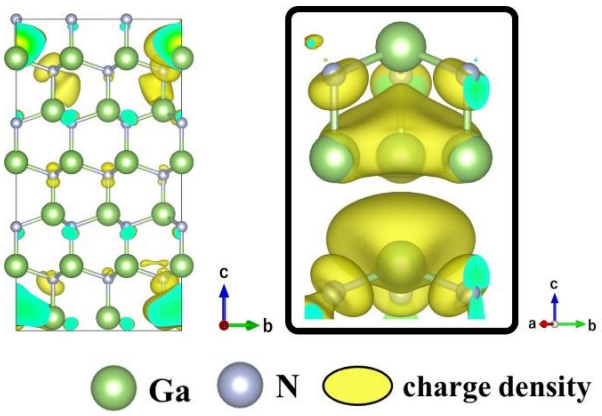

Fig. 9. Defect level at the Γ point of the defect model. The isosurface values were taken as 0.001/bohr^3.

Fig. 10 shows the charge density distributions of the F3p2_opt model at the Γ point (orange and blue points in Fig. 7(c)), which correspond to the lowest unoccupied state and highest occupied state, respectively. Fig. 10(a) shows that the charge density of the CBM is distributed around the N atoms with an s-orbital-like shape, while Fig. 10(b) shows that the charge density of the VBM is distributed around the N atoms with an p-orbital-like shape, similar to the defect-free model. In addition, no localized states are observed in the lowest unoccupied state and highest occupied state, indicating that placing three F atoms around the N vacancy terminates the Ga dangling bonds and results in a state that closely resembles that of a defect-free GaN crystal. The peaks of the PDOS for the Ga 4p orbitals and F 2p orbitals overlap near an energy of −7.5 eV (lower left panel in Fig 7(c)), which suggests a bond between the Ga dangling bonds and F atoms. Fig. 10(c) shows that the charge density distribution of the bonding state is localized around the F atoms and the Ga atoms adjacent to the N vacancy. This indicates that the Ga atoms adjacent to the N vacancy bond with the F atoms, resulting in elimination of the defect level.

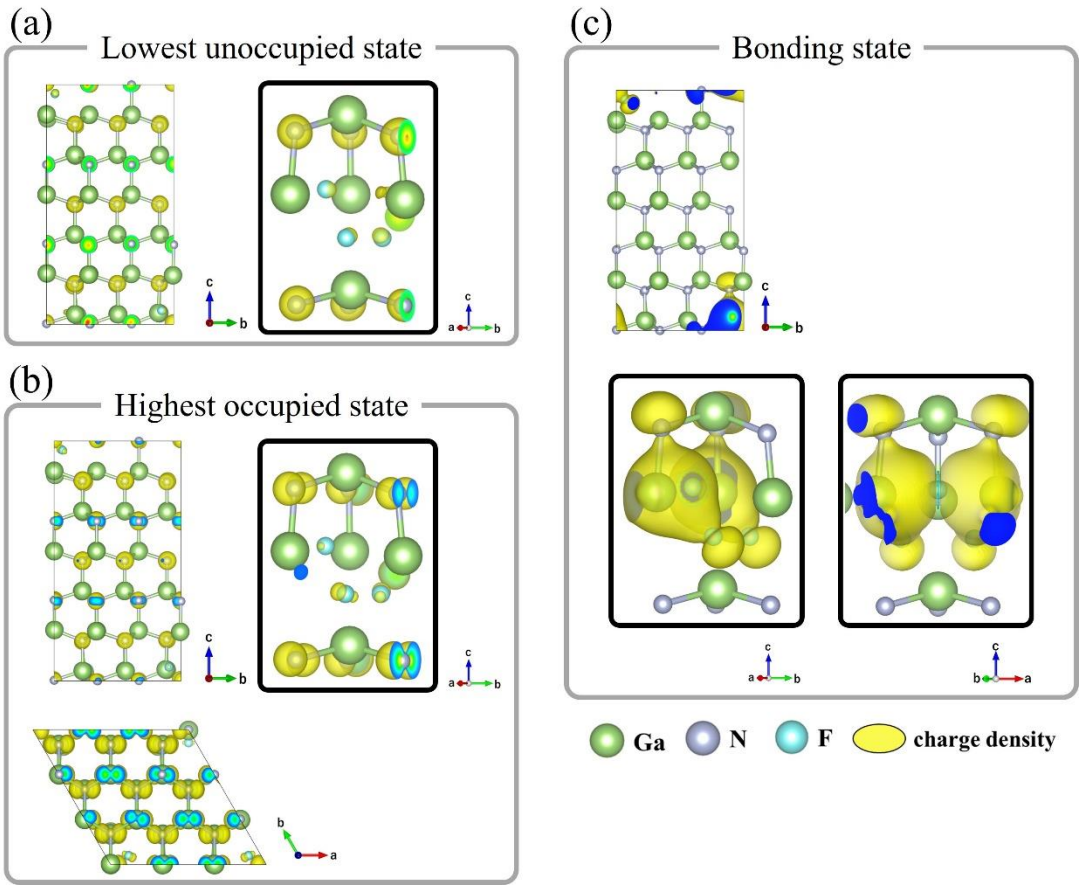

Fig. 10. Charge density distributions of the F3p2_opt model: (a) lowest unoccupied state, (b) highest occupied state, and (c) bonding state. The isosurface values were taken as 0.001/bohr^3.

Unlike the band dispersion diagram of the defect-free model (Fig. 7(a)), the band dispersion diagram of the H3p2_opt model (Fig. 7(d)) has a band near an energy of 0 eV. The PDOS of the H3pt_opt model (Fig. 7(d)) also has an overlap between Ga atoms adjacent to the N vacancy and H atoms near the VBM around an energy of 0 eV, which suggests bonding between the Ga dangling bonds and H atoms. Fig. 11(b) shows that the charge density distribution of the highest occupied state at the Γ point (pink point in Fig. 7(d)) is localized around the H atoms and Ga atoms adjacent to the N vacancy, suggesting that this state corresponds to the bonding between the Ga dangling bonds and 1s orbitals of the H atoms. These results indicate that similar to F termination, H termination leads to bonding between Ga dangling bonds and H atoms.

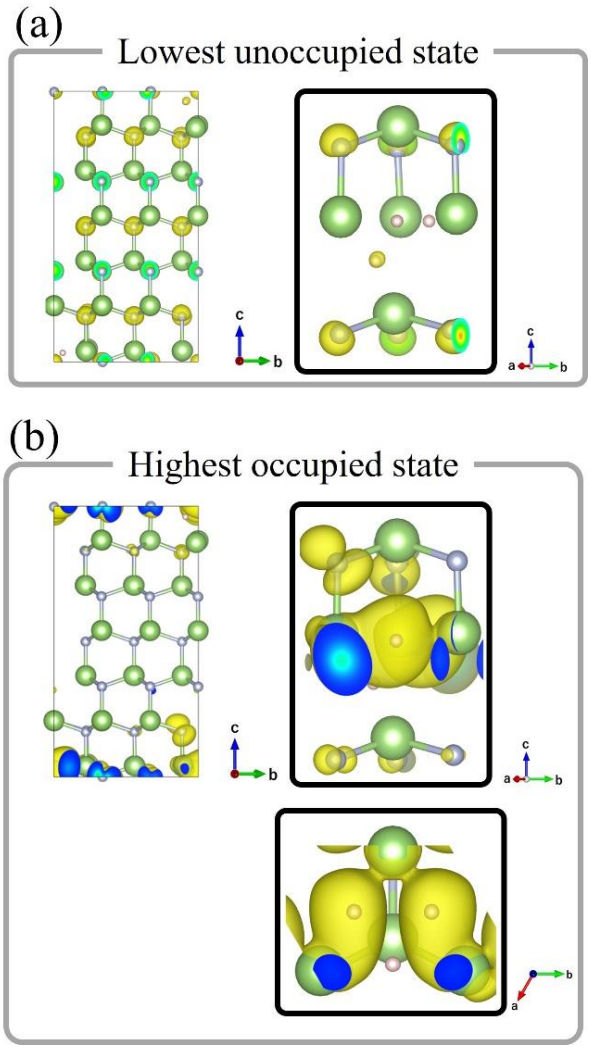

Fig. 11. Charge density distributions of the H3p2_opt model: (a) lowest unoccupied state and (b) highest occupied state. The isosurface values were taken to be 0.001/bohr^3.

C. Difference between F and H termination

The results in the previous section indicated that F termination is more effective than H termination at eliminating defect levels near the band edges because it shifts these defective states to energy levels far from the band edges. This difference may be attributed to the larger energy difference between the bonding and antibonding states induced by F termination compared to that induced by H termination. The energy eigenvalues for the Ga 4p, F 2p, and H 1s orbitals were calculated to be −5.673573, −19.86485 and −13.60569 eV, respectively, by Harada using the self-consistent field method within the Hartree–Fock approximation.[36] Thus the F 2p orbital has a lower energy than the H 1s orbital. Fig. 12 shows a schematic of how the energy difference between the bonding and antibonding states induced by binding between the Ga dangling bonds primarily comprising Ga 4p orbitals and F 2p

orbital is larger than the case with the H 1s orbital. This energy difference means that the adsorption of H onto Ga dangling bonds results in the bonding state remaining near the band edges. In contrast, the adsorption of F onto Ga dangling bonds results in a bonding state that forms at an energy level far from the band edges. This results in electronic states near the band edge resembling those of defect-free GaN. In other words, F termination eliminates defect levels more effectively and can improve the performance of GaN-based devices.

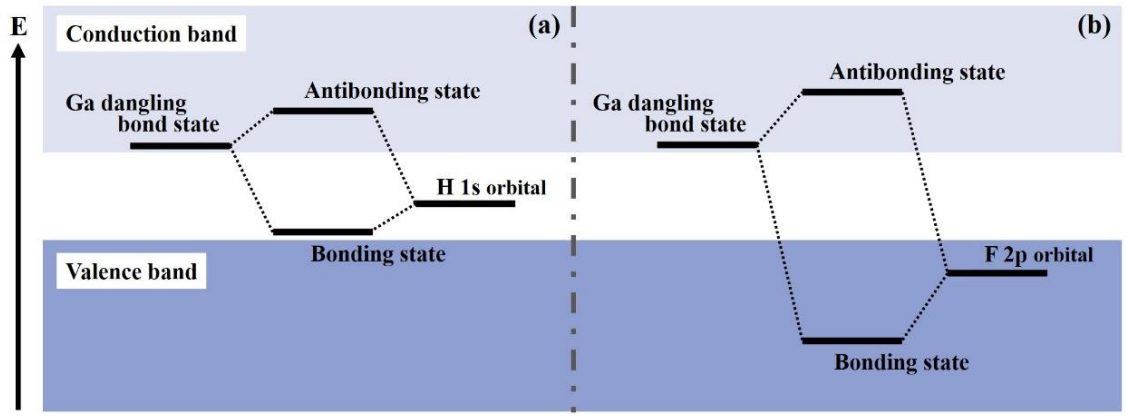

Fig. 12. Schematic of the differences in energy of the bonding and antibonding states with (a) H termination and (b) F termination.

IV. Conclusion

We used first-principles calculations to investigate the atomic configurations in which three F or H atoms are adsorbed onto Ga dangling bonds inside GaN crystals and the electronic states. For F termination, the most stable configuration corresponded to three F atoms adsorbed at low-symmetry sites located farther from the Ga atoms. In contrast, the most stable atomic configuration for H termination was with three H atoms at positions closer to the Ga atoms. F termination eliminated defect levels near the band edges by forming bonds between the Ga dangling bonds and F atoms, resulting in electronic states similar to those of defect-free GaN. In contrast, although H termination also formed bonds between Ga dangling bonds and the H atoms, the resulting bonding state appeared near the VBM. The localized states induced by H termination could affect the performance of GaN-based devices. While this study does not address experimental methods of F incorporation, the findings indicate that achieving an ideal fluorinated configuration could effectively eliminate defect levels.

SUPPLEMENTARY MATERIAL

The formation energies of F-terminated models with one to four F atoms placed around the N vacancy are compared.

ACKNOWLEDGMENTS

This work was supported by JSPS KAKENHI Grant Number 25K08496 and used computational resources of AOBA-S provided by Tohoku University through the HPCI System Research Project (Project ID: hp250045).

AUTHOR DECLARATIONS

Conflict of interest

The authors have no conflicts to disclose.

Author contributions

Y. Fujishiro: Data Curation (lead). Formal Analysis (lead). Investigation (lead). Methodology (equal). Visualization (lead). Writing–Original Draft Preparation (lead). **T. Yayama**: Conceptualization (lead). Data Curation (support). Funding Acquisition (lead). Investigation (support). Methodology (equal). Project Administration (support). Resources (equal). Software (equal). Validation (equal). Writing–Original Draft Preparation (support). **T. Nagata**: Conceptualization (equal). Validation (equal). Writing–Review & Editing (equal). **T. Chikyow**: Conceptualization (equal). Validation (equal). Writing–Review & Editing (equal). **F. Akagi**: Project Administration (lead). Resources (equal). Software (equal). Supervision (lead). Validation (equal). Writing–Review & Editing (equal).

Data availability

The data that support the findings of this study are available within the article.

REFERENCES

[1]H. Amano, Y. Baines, E. Beam, M. Borga, T. Bouchet, P. R. Chalker, M. Charles, K. J. Chen, N. Chowdhury, R. Chu, C. D. Santi, M. M. D. Souza, S. Decoutere, L. D. Cioccio, B. Eckardt, t. Egawa, P. Gay, J. J. Freedsman, L. Guido, O. Häberlen, g. Haynes, T. Heckel, D. Hemakumara, P. Houston, J. Hu, M. Hua, Q. Huang, A. Huang, S. Jiang, H. Kawai, D. Kinzer, M. Kuball, A. Kumar, K. B. Lee, X. Li, D. Marcon, M. März, R. McCarthy, G. Meneghesso, M. Meneghini, E. Morvan, A. Nakajima, E. M. S. Narayanan, S. Oliver, T. Palacios, D. Piedra, M. Plissonnier, R. Reddy, M. Sun, I. Thayne, A. Torres, N. Trivellin, V. Unni, M. J. Uren, M. V. Hove, D. J. Wallis, J. Wang, J. Xie, S. Yagi, S. Yang, C. Youtsey, R. Yu, E. Zanoni, S. Zeltner, and Y. Zang, J. Phys. D: Appl. Phys. 51, 163001 (2018).

[2]T. Oka, Jpn. J. Appl. Phys. Part 1 58, SB0805 (2019).

[3]S. J. Pearton, J. C. Zolper, R. J. Shul, and F. Ren, J. Appl. Phys. 86, 1 (1999).

[4]P. B. Klein, J. A. Freitas, Jr., S. C. Binari, and A. E. Wickenden, Appl. Phys. Lett. 75, 4016 (1999).

[5]C.G. Van de Walle, Phys. Rev. B 49, 4579 (1994).

[6]R. Okuyama, T. Kadono, S. Shigematsu, A. Onaka-Masada, A. Suzuki, K. Kobayashi, R. Hirose, Y. Koga, and K. Kurita, Jpn. J. Appl. Phys. 59, 125502 (2020).

[7]E. Bruno, S. Mirabella, G. Impellizzeri, F. Priolo, F. Giannazzo, V. Raineri, and E. Napolitani, Appl. Phys. Lett. 87, 133110 (2005).

[8]H. Boo, J.-H. Lee, M. G. Kang, K. D. Lee, S. Kim, H. C. Hwang, W. J. Hwang, H. O. Kang, S. Park, S. J. Tark, and D. Kim, Int. J. Photoenergy. 2012, 921908 (2011).

[9]J. C. Zolper, H. H. Tan, J. S. Williams, J. Zou, D. J. H. Cockayne, S. J. Pearton, M. Hagerott Crawford, and R. F. Karlicek Jr., Appl. Phys. Lett. 70, 2729 (1997).

[10]H. Sakurai, M. Omori, S. Yamada, Y. Furukawa, H. Suzuki, T. Narita, K. Kataoka, M. Horita, M. Bockowski, J. Suda, and T. Kachi, Appl. Phys. Lett. 115, 142104 (2019).

[11]J. S. Williams, Mater. Sci. Eng. A 253, 8 (1998).

[12]J. C. Zolper, J. Cryst. Growth 178, 157 (1997).

[13]H. Sakurai, T. Narita, M. Omori, S. Yamada, A. Koura, M. Iwinska, K. Kataoka, M. Horita, N. Ikarashi, M. Bockowski, J. Suda, and T. Kachi, Appl. Phys. Express 13, 086501 (2020).

[14]Y. Wada, H. Mizobata, T. Shimura, M. Nozaki, T. Kobayashi, and H. Watanabe, Appl. Phys. Lett. 120, 082103 (2022).

[15]S. Y. Nishath, K. Singh, and S. Pal, Phys. Status Solidi A 2500047 (2025).

[16]A. Castiglia, J.-F. Carlin, and N. Grandjean, Appl. Phys. Lett. 98, 213505 (2011).

[17]S. Nakamura, N. Iwasa, M. Senoh, and T. Mukai, Jpn, J. Phys. 31, 1258 (1992).

[18]W.-S. Jung, J.-H. Park, A. Nainani, D. Nam, and K. C. Saraswat, Appl. Phys. Lett. 101, 072104 (2012).

[19]M. J. Wang, L. Yuan, K. J. Chen, F. J. Xu, and B. Shen, J. Appl. Phys. 105, 083519 (2009).

[20]L. Yuan, M. J. Wang, and K. J. Chena, J. Appl. Phys. 104, 116106 (2008).

[21]T. Nagata, A. Matsuda, T. Teramoto, D. Gerlach, P. Shen, S. Ueda, T, Kimura, C. Dussarrat, and T. Chikyow, J. Appl. Phys. 137, 095304 (2025).

[22]A. Matsuda, T. Teramoto, T. Nagata, D. Gerlach, P. Shen, S. Ueda, T, Kimura, C. Dussarrat, and T. Chikyow, Appl. Surf. Sci. 659, 159941 (2024).

[23]Z. Gao, B. Hou, Y. Liu, X. Ma, Microelectron. Eng. 154, 22 (2016).

[24]T. Yayama, N. Iba, T. Nagata, T. Chikyow, The 14th. International Conference on Nitrides Semiconductors, Poster, MoP-CH-32 (2023).

[25]G. Kresse and J. Hafner, Phys. Rev. B 48, 13115 (1993).

[26]G. Kresse and J. Furthmüller, Phys. Rev. B 54, 11169 (1996).

[27]G. Kresse and J. Furthmüller, Comput. Mater. Sci. 6, 15 (1996).

[28]J. Hafner, Comput. Phys. Commun. 177, 6 (2007).

[29]J. P. Perdew, K. Burke, and M. Ernzerhof, Phys. Rev. Lett. 77, 3865 (1996).

[30]J. P. Perdew, M. Ernzerhof, and K. Burke, J. Chem. Phys. 105, 9982 (1996).

[31]M. Ernzerhof and G. Scuseria, J. Chem. Phys. 110, 5029 (1999).

[32]J. L. Lyons, C. G. Van de Walle, npj Comput. Mater. 3, 12 (2017).

[33]M. D. Pashley, Phys. Rev. B 40, 10481 (1989).

[34]Q. S. Zhu and N. Sawaki, Appl. Phys. Lett. 76, 1594 (2000).

[35]D. K. Lewis, M. Matsubara, E. Bellotti, and S. Sharifzadeh, Phys. Rev. B 96, 235203 (2017).

[36]F. Y. Harada, Quantum Chemistry, Vol. 1, 211, SHOKABO Co., Ltd (2007).